Richards Tests

Andy Wilkins
CSIRO

January 3, 2014

Contents

1 Introduction

The Richards' equation describes slow fluid flow through a porous medium. This document describes the test suite associated with the Richards MOOSE code: both brief unit-style tests, and more complicated benchmark verifications. Many of the tests are run automatically every time the code is updated. Some of the tests are marked 'heavy' since they are more lengthy (they take over 2 seconds to run) and these must be run manually. There are two other accompanying documents: (1) The theoretical and numerical foundations of the code, which also describes the notation used throughout this document; (2) Examples of input syntax that users can utilise when building models.

The test suite does not *prove* that the Richards' equation is correctly implemented in MOOSE, as the expected results might be obtained by pure luck. The tests are ordered approximately by complexity, so that by the end I hope that all readers will agree that the implementation is highly likely to be correct. The tests are as follows.

- Chapter 2 tests the so-called UserObjects that define the Richards' nonlinear functions: relative permeability, density, and effective saturation. These functions are independent of the Darcy/Richards flow, but of course they must be correctly implemented in order that the code give correct solutions of flow problems.
- Chapter 3 contains many tests the Jacobian of Richards' flow. The Jacobian actually has little effect on the final numerical solution of a flow problem, but if it is incorrectly implemented then MOOSE will display poor convergence characteristics. Therefore it is extremely important to check the Jacobian.
- Chapter 4 contains many tests of the long-time behaviour in simple problems, which should just be hydrostatic pressure head, with the caveat that $S \geq S_{\rm imm}$.
- Chapter 5 checks that pressure pulses diffuse correctly through a fully-saturated medium. For readers experienced in the groundwater, this is very similar to the Theis solution.
- Chapter 6 checks that MOOSE behaves correctly when the system contains a sink flux that is a function of porepressure. A particular function is used so that an analytic solution exists.
- Chapter 7 demonstrates that flow in the unsaturated region along with source fluxes is correctly implemented by comparing with the analytic solution of Broadbridge and White for constant infiltration.
- Chapter 8 demonstrates that flow in the unsaturated region is correctly implemented by comparing with the analytic solution of Warrick, Lomen and Islas for drainage of a medium under the action of gravity.

- Chapter 9 compares MOOSE with numerical results from HYDRUS for infiltration and drainage from a large caisson. In reality, this is very similar to Chapters 7 and 8: the only essential differences are the capillary and relative permeability functions.
- Chapter 10 compares MOOSE with the analytic solution of the Buckley-Leverett problem.

2 UserObject tests

The Richards' UserObjects define the nonlinear functions that form the core of all models. The tests of these UserObjects involve checking whether the functions and their derivatives are correctly coded. This is done by comparing the values of the UserObjects with ParsedFunctions that are coded into a MOOSE input file, and the values of the UserObject derivatives with finite-differences of the same ParsedFunction. These are simple tests and are part of the automatic test suite. The following tests are performed.

- That the 'power' form of the relative permeability:

$$\kappa_{\rm rel}(S) = (n+1)S^n - nS^{n+1} \ , \tag{2.1}$$

  is correctly coded, and also that its first and second derivatives with repsect to S are correctly coded.

- That the 'van Genuchten' form of the relative permeability:

$$\kappa_{\rm rel}(S) = \sqrt{S}\left(1-\left(1-S^{1/m}\right)^m\right)^2 \ , \tag{2.2}$$

  is correctly coded, and also that its first and second derivatives with respect to S are correctly coded.

- That the 'modified van Genuchten' form of the relative permeability:

$$\kappa_{\rm rel}(S) = \begin{cases} \sqrt{S}\left(1-\left(1-S^{1/m}\right)^m\right)^2 & \text{for } S < S_{\rm cut} \\ \text{cubic} & \text{for } S \geq S_{\rm cut} \end{cases} \tag{2.3}$$

  is correctly coded, and also that its first and second derivatives with respect to S are correctly coded.

- That the 'Broadbridge-White' form of the relative permeability:

$$\kappa_{\rm rel}(S) = \kappa_n + (\kappa_s - \kappa_n)\frac{\Theta^2(C-1)}{C-\Theta} \ , \tag{2.4}$$

  where $\Theta = (S-S_n)/(S_s-S_n)$, is correctly coded, and also that its first and second derivatives with respect to S are correctly coded. Broadbridge and White assume that saturation is bounded $S_n \leq S \leq S_s$, so for most MOOSE models it is appropriate to treat S_n as the immobile saturation with $\kappa_n = 0$, and $S_s = 1$ with $\kappa_s = 1$.

- That the 'constant bulk modulus' form of the density

$$\rho(P) = \rho_0 e^{P/B} \ , \tag{2.5}$$

  is correctly coded, and also that its first and second derivatives with respect to P are correctly coded.

- That the 'ideal gas' form of the density

$$\rho(P) = s(P - P_0) \ , \tag{2.6}$$

  is correctly coded, and also that its first and second derivatives with respect to P are correctly coded.

- That the 'van Genuchten' effective saturation

$$S_{\rm eff} = \left(1 + (\alpha P_{\rm c})^{\frac{1}{1-m}}\right)^{-m} \ , \tag{2.7}$$

  is correctly coded, and also that its first and second derivatives with respect to $P_{\rm c}$ are correctly coded.

- That the 'Broadbridge-White' effective saturation valid for small κ_n, defined by

$$\frac{P_{\rm c}}{\lambda_s} = \frac{1-\Theta}{\Theta} - \frac{1}{C}\log\left(\frac{C-\Theta}{(C-1)\Theta}\right) \ , \tag{2.8}$$

  with $\Theta = (S_{\rm eff} - S_n)/(S_s - S_n)$, is correctly coded, and also that the first and second derivatives of $S_{\rm eff}$ with respect to $P_{\rm c}$ are correctly coded. Note that Broadbridge and White assume that $S_{\rm eff} = S$ (no residual saturations) and $S_n \leq S \leq S_s$, so in most MOOSE models S_n is the immobile saturation.

3 Jacobian tests

The UserObjects and their derivatives need to be combined to form a residual and a Jacobian during the solution process. Correctly coding the Jacobian leads to rapid convergence to the correct solution, so tests of the Jacobian are important. These are simple tests and are part of the automatic test suite.

In MOOSE parlance, the Jacobian consists of 'Diagonal' and 'OffDiagonal' terms. The former consist of the derivative of a variable's residual with respect to the same variable (at the same quadrature point or a different one); while the latter consist of the derivatives with respect to another variable (at the same quadrature point or a different one).

The 'Diagonal' terms are tested using a single-phase single-element model with random initial conditions. Sixteen different tests are performed which are all possible combinations of:

- Fully-saturated or unsaturated initial conditions
- With or without gravity
- With or without SUPG
- With or without time derivatives

Of course, the unsaturated case with gravity, SUPG and time derivatives is the most complicated, but the other cases are useful for debugging.

The 'OffDiagonal' terms only appear if there is more than one pressure variable, that is for multi-phase problems. No tests have been performed yet.

4 Long-time behaviour

These tests concern the steadystate pressure distribution obtained either by running a transient model for a long time, or by running a steady-state analysis, both of which should lead to the same result. Without fluxes, the steadystate pressure distribution is just

$$P(x) = P_0 + \rho_0 g x \,, \tag{4.1}$$

if the fluid bulk modulus is large enough compared with P. Here ρ_0 is the constant reference fluid density, g is the acceleration due to gravity (a vector), and x is position. These are simple tests and are part of the automatic test suite.

This is verified by running sixteen single-phase single-element models with random initial conditions. The sixteen cases are all possible combinations of:

- Fully-saturated or unsaturated initial conditions
- With or without gravity
- With or without SUPG
- Transient or Steadystate

In addition to these cases, a number of more complicated scenarios are also part of the automatic test suite:

1. A single-phase situation with nonzero immobile saturation. There are 5 elements in the x direction along which gravity acts. The x direction has length 20 m, and the initial condition is sufficiently unsaturated so that after some time the saturation at the 'top' of the model ($x \sim 20$) would reduce below immobile saturation if the relative permeability weren't preventing it. Two cases are studied: with SUPG and without SUPG. The results are shown in the top two pictures of Figure 4.1 and show that SUPG reduces oscillations and prevents $S < S_{\rm imm}$ in this example at least.

2. The same situation is in item 1, but with 50 elements in the x direction. Figure 4.1 shows once again the stabilising nature of SUPG is seen, as well as the hydrostatic pressure head for $S > S_{\rm imm}$.

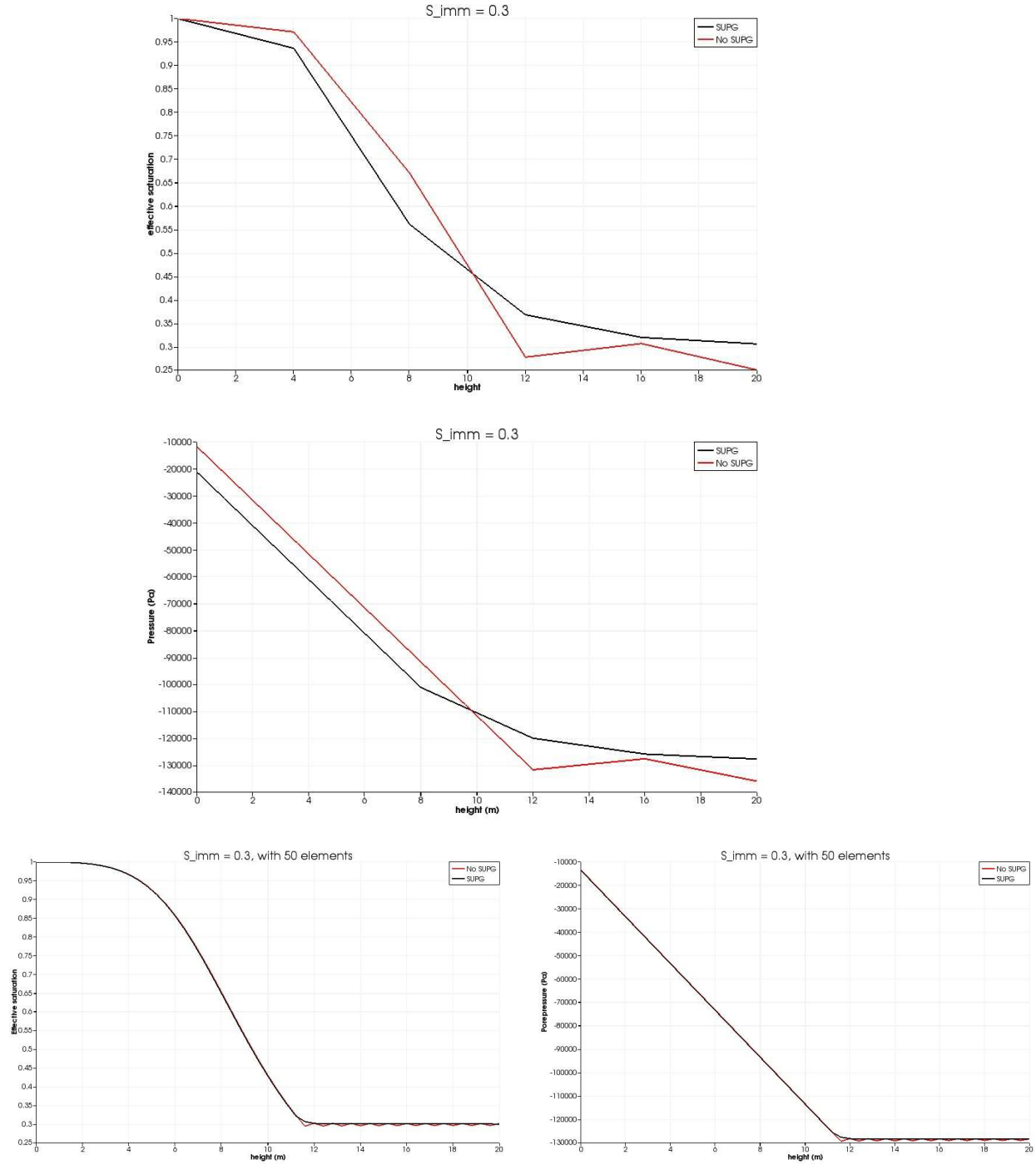

Figure 4.1: Results for $S_{\text{imm}} = 0.3$. Gravity points to the left. Top picture: Effective saturation. Middle picture: Pore pressure. Bottom pictures: The situation with 50 elements in the x direction instead of just 5. In each picture the red line is without SUPG, and oscillatory results can be observed in addition to $S_{\text{eff}} < S_{\text{imm}}$.

5 A pressure pulse in the fully saturated situation

Richards' equation for flow through a fully saturated medium without gravity and without sources is just Darcy's equation

$$\frac{\partial}{\partial t}\phi\rho = \nabla_i \left(\frac{\rho\kappa_{ij}}{\mu}\nabla_j P \right) , \tag{5.1}$$

with notation described in the Theory Manual. Using $\rho \propto \exp(P/K)$, where K is the fluid bulk modulus, Darcy's equation becomes

$$\frac{\partial}{\partial t}\rho = \nabla_i \alpha_{ij} \nabla\rho , \tag{5.2}$$

with

$$\alpha_{ij} = \frac{\kappa_{ij}B}{\mu\phi} . \tag{5.3}$$

Here I've assumed the porosity and bulk modulus are constant in space and time.

Consider the one-dimensional case were the spatial dimension is the semi-infinite line $x \geq 0$. Suppose that initially the pressure is constant, so that

$$\rho(x, t = 0) = \rho_0 \quad \text{for} \quad x \geq 0 . \tag{5.4}$$

Then apply a fixed-pressure Dirichlet boundary condition at $x = 0$ so that

$$\rho(x = 0, t > 0) = \rho_\infty \tag{5.5}$$

The solution of the above differential equation is well known to be

$$\rho(x,t) = \rho_\infty + (\rho_0 - \rho_\infty)\,\mathrm{Erf}\left(\frac{x}{\sqrt{4\alpha t}} \right) , \tag{5.6}$$

where Erf is the error function.

This is verified by using the following two tests on a line of 10 elements.

1. Steady state analysis to demonstrate that the steady-state of $\rho = \rho_\infty$ is achieved.
2. Transient analysis

An example verification is shown in Figure 5.1. These tests run rapidly and are part of the automatic test suite.

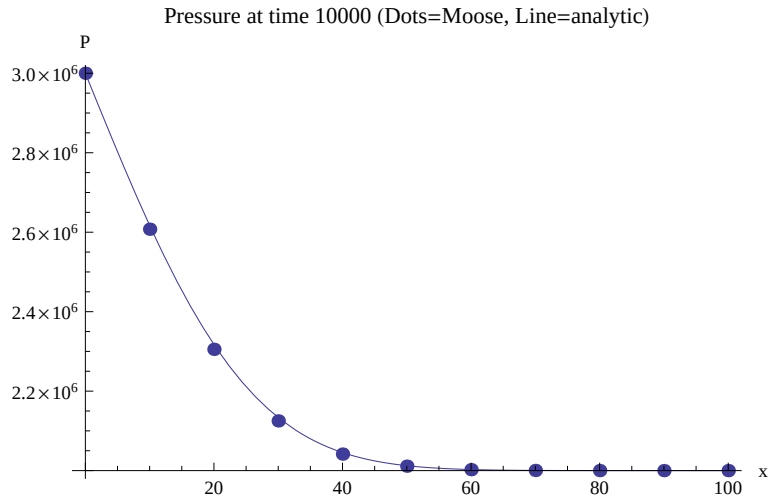

Figure 5.1: Comparison between the MOOSE result (in dots), and the exact analytic expression given by Eqn (5.6). This test had 10 elements in the x direction, with $0 \leq x \leq 100\,\mathrm{m}$, and ran for a total of 10^4 seconds with 10 timesteps. The parameters were $B = 2\,\mathrm{GPa}$, $\kappa_{xx} = 10^{-15}\,\mathrm{m}^2$, $\mu = 10^{-3}$ Pa.s, $\phi = 0.1$, with initial pressure $P = 2\,\mathrm{MPa}$, and applied pressure $P = 3\,\mathrm{MPa}$ at $x = 0$. For greater spatial resolution and smaller timesteps the agreement increases.

6 Newton cooling from a bar

This test demonstrates that MOOSE behaves correctly when a simulation contains a sink. The sink is a piecewise linear function of pressure.

Darcy's equation for flow through a fully saturated medium without gravity and without sources is

$$\frac{\partial}{\partial t}\phi\rho = \nabla_i\left(\frac{\rho\kappa_{ij}}{\mu}\nabla_j P\right) , \tag{6.1}$$

with notation described in the Theory Manual. Using $\rho \propto \exp(P/K)$, where K is the fluid bulk modulus, Darcy's equation becomes

$$\frac{\partial}{\partial t}\rho = \nabla_i\alpha_{ij}\nabla\rho , \tag{6.2}$$

with

$$\alpha_{ij} = \frac{\kappa_{ij}B}{\mu\phi} . \tag{6.3}$$

Here I've assumed the porosity and bulk modulus are constant in space and time.

Consider the one-dimensional case where a bar sits between $x = 0$ and $x = L$ with initial pressure distribution so $\rho(x,t=0) = \rho_0(x)$. Maintain the end $x = 0$ at constant pressure, so that $\rho(x=0,t) = \rho_0(0)$. At the end $x = L$, prescribe a sink flux

$$\left.\frac{\partial\rho}{\partial x}\right|_{x=L} = -C\left(\rho-\rho_e\right)_{x=L} , \tag{6.4}$$

where ρ_e is a fixed quantity ("e" stands for "external"), and C is a constant conductance. This corresponds to the flux

$$\left.\frac{\partial P}{\partial x}\right|_{x=L} = -CB\left(1-e^{(P_e-P)/B}\right)_{x=L} , \tag{6.5}$$

which can easily be coded into a MOOSE input file: the flux is $\rho\kappa\nabla P/\mu = -CB\kappa(e^{P/B} - e^{P_e/B})/\mu$, and this may be represented by a piecewise linear function of pressure.

The solution of this problem is well known and is

$$\rho(x,t) = \rho_0(0) - \frac{\rho_0(0)-\rho_e}{1+LC}Cx + \sum_{n=1}^{\infty} a_n \sin\frac{k_n x}{L} e^{-k_n^2\alpha t/L^2} , \tag{6.6}$$

where k_n is the n^{th} positive root of the equation $LC\tan k + k = 0$ (k_n is a little bigger than $(2n-1)\pi/2$), and a_n is determined from

$$a_n\int_0^L \sin^2\frac{k_n x}{L}\,\mathrm{d}x = \int_0^L\left(\rho_0(x)-\rho_0(0)+\frac{\rho_0(0)-\rho_e}{1+LC}Cx\right)\sin\frac{k_n x}{L}\,\mathrm{d}x , \tag{6.7}$$

which may be solved numerically (I have used Mathematica to generate the solution in Figure 6.1).
The problem is solved in MOOSE using the following parameters:

Bar length	100 m
Bar porosity	0.1
Bar permeability	10^{-15} m^2
Gravity	0
Water density	1000 kg.m^{-3}
Water viscosity	0.001 Pa.s
Water bulk modulus	1 MPa
Initial porepressure P_0	2 MPa
Environmental pressure P_e	0
Conductance C	0.05389 m^{-1}

This conductance is chosen so at steadystate $\rho(x = L) = 2000\,\text{kg.m}^{-3}$.

The problem is solved using 1000 elements along the x direction ($L = 100$ m), and using 100 time-steps of size 10^6 s. Using fewer elements or fewer timesteps means the agreement with the theory is marginally poorer. The problem is also solved using the steadystate solver. In this case the initial condition is $P = 2 - x/L$ MPa, since the uniform $P = 2$ MPa does not converge. The results are shown in Figure 6.1.

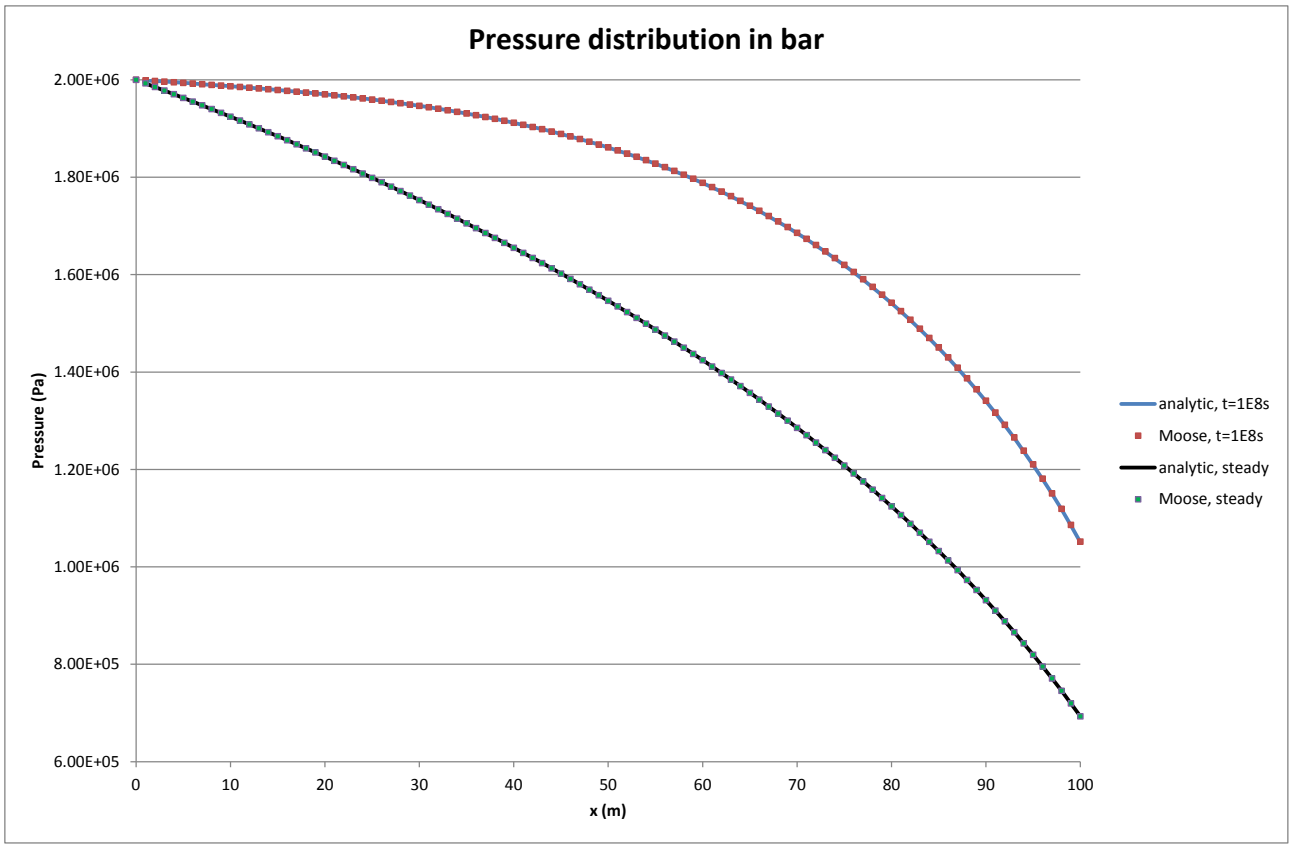

Figure 6.1: The porepressure in the bar at $t = 10^8$ s, and at steadystate. The pressure at $x = 0$ is held fixed, while the sink is applied at $x = 100$ m. MOOSE agrees well with theory demonstrating that piecewise-linear sinks/sources are correctly implemented in MOOSE.

7 The analytic infiltration solution

The Richards' equation for an incompressible fluid reads in one spatial dimension (z) reads

$$\dot{S} = \nabla\left(D\nabla S\right) - \nabla K \ , \tag{7.1}$$

where

$$D(S) = -\frac{\kappa\kappa_{rel}}{\mu\phi}P_{\rm c}' \ , \tag{7.2}$$

$$K(S) = \frac{\rho g\kappa\kappa_{\rm rel}}{\mu\phi} \ . \tag{7.3}$$

Here $P_{\rm c} = -P$ which is the capillary pressure, and recall that $P_{\rm c}'(S) < 0$.

The analytic solution of this nonlinear diffusion-advection relevant to constant infiltration to groundwater has been derived Broadbridge and White[1] for certain functions D and K. The setup is shown in "Experiment 1" of Figure 9.1 (ignore the specified infiltration rate, initial saturation and height of sample). Broadbridge and White assume the hydraulic conductivity is

$$K(S) = K_n + (K_s - K_n)\frac{\Theta^2(C-1)}{C-\Theta} \ , \tag{7.4}$$

where

$$\Theta = \frac{S - S_n}{S_s - S_s} \ , \tag{7.5}$$

and the parameters obey $0 \le K_n < K_s$, $0 \le S_n \le S \le S_s \le 1$, and $C > 1$. The diffusivity is of the form $a(b-S)^{-2}$. This leads to very complicated relationships between the capillary pressure, P_c, and the saturation, except in the case where K_n is small, when they are related through

$$\frac{P_{\rm c}}{\lambda_s} = \frac{1-\Theta}{\Theta} - \frac{1}{C}\log\left(\frac{C-\Theta}{(C-1)\Theta}\right) \ , \tag{7.6}$$

with $\lambda_{\rm s} > 0$ being the final parameter.

Broadbridge and White derive time-dependent solutions for constant recharge to one end of a semi-infinite line. This represents constant rainfall recharge to an initially unsaturated soil block, for instance. Their solutions are quite lengthy, so I will not write them here. To compare with MOOSE, I use the following parameters — the hydraulic parameters are those used in Figure 3 of Broadbridge and White:

[1] P Broadbridge, I White "Constant rate rainfall infiltration: A versatile nonlinear model, 1 Analytical solution". Water Resources Research 24 (1988) 145–154.

Bar length	20 m
Bar porosity	0.25
Bar permeability	1
Gravity	$0.1\,\mathrm{m.s^{-2}}$
Fluid density	$10\,\mathrm{kg.m^{-3}}$
Fluid viscosity	4 Pa.s
S_n	$0\,\mathrm{m.s^{-1}}$
S_s	$1\,\mathrm{m.s^{-1}}$
K_n	$0\,\mathrm{m.s^{-1}}$
K_s	$1\,\mathrm{m.s^{-1}}$
C	1.5
λ_s	2 Pa
Recharge rate R_*	0.5

Broadbridge and white consider the case where the initial condition is $S = S_s$, but this yields $P = -\infty$, which is impossible to use in a MOOSE model. Therefore the initial condition $P = -900\,\mathrm{Pa}$ is used which avoids any underflow problems. The recharge rate of $R_* = 0.5$ corresponds in the MOOSE model to a recharge rate of $0.5\rho\phi(\kappa_s - \kappa_n) = 1.25\,\mathrm{kg.m^{-2}.s^{-1}}$. Note that I've chosen $\frac{\rho g \kappa}{\mu\phi} = 1\,\mathrm{m.s^{-1}}$, so that the K_n and K_s may be encoded as $\kappa_n = 0$ and $\kappa_s = 1$ in the relative permeability function Eqn (2.4) in a straightforward way.

Figure 7.1 shows good agreement between the analytic solution of Broadbridge and White and the MOOSE implementation. There are minor discrepancies for small values of saturation: these get smaller as the temporal and spatial resolution is increased, but never totally disappear due to the initial condition of $P = -900\,\mathrm{Pa}$.

This test is part of the automatic test suite that is run every time the code is updated.

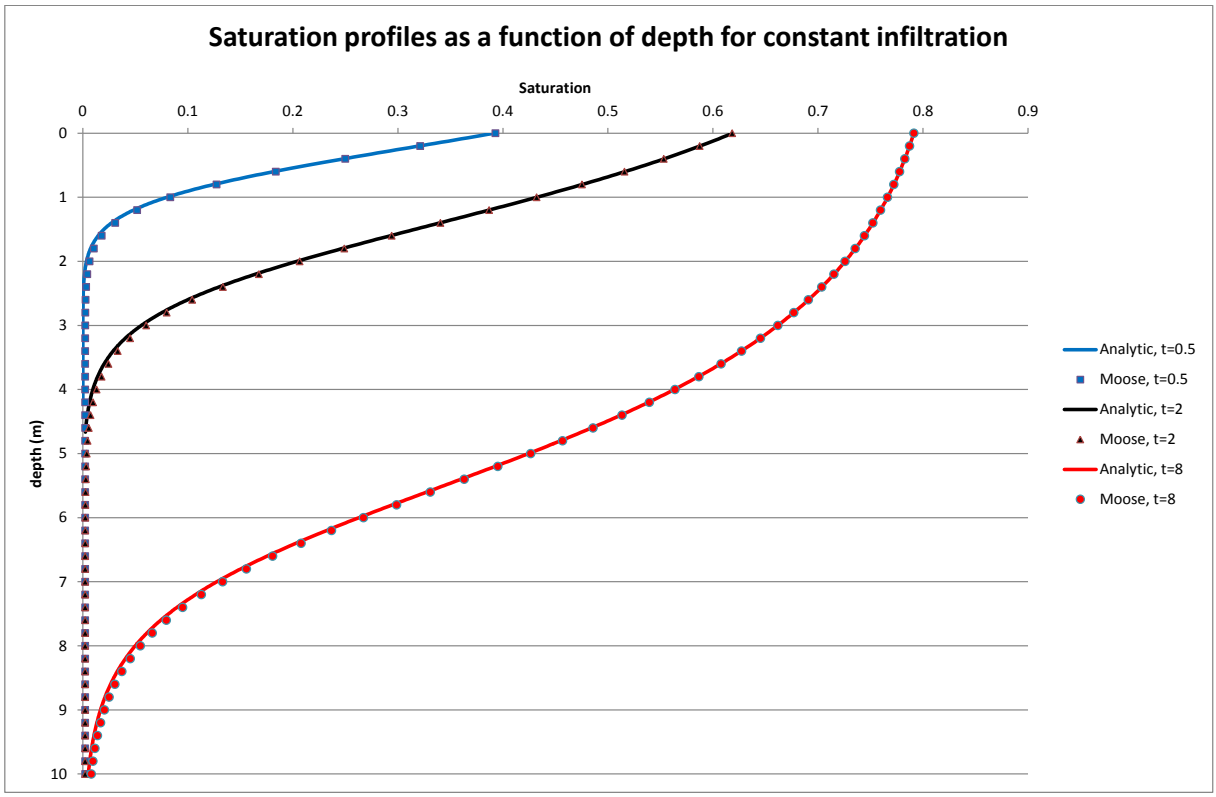

Figure 7.1: Comparison of the Broadbridge and White analytical solution with the MOOSE solution for 3 times. This figure is shown in the standard format used in the Broadbridge-White paper: the constant recharge is applied to the depth = 0 surface, and gravity acts downwards in this figure.

8 The analytic drainage solution

Warrick, Lomen and Islas[1] extended the analysis of Broadbridge and White (Chapter 7) to include the case of drainage from a medium. The setup is in "Experiment 2" of Figure 9.1. To obtain their analytical solutions, Warrick, Lomen and Islas make the same assumptions as Broadbridge and White concerning the diffusivity and conductivity of the medium. Their solutions are quite lengthy, so I will not write them here.

A MOOSE model with the parameters almost identical to those listed in Chapter 7 is compared with the analytical solutions. The only differences are that the "bar" length is 10000 m (to avoid any interference from the lower Dirichlet boundary condition), and $R_* = 0$ since there is no recharge. The initial condition is $P = 10^{-4}$ Pa: the choice $P = 0$ leads to poor convergence since by construction the Broadbridge-White capillary function is only designed to simulate the unsaturated zone $P < 0$ and a sensible extension to $P \geq 0$ is discontinuous at $P = 0$.

Figure 8.1 shows good agreement between the analytic solution and the MOOSE implementation. Any minor discrepancies get smaller as the temporal and spatial resolution increase.

This test is part of the automatic test suite that is run every time the code is updated.

[1] AW Warrick, DO Lomen and A Islas, "An analytical solution to Richards' Equation for a Draining Soil Profile", Water Resources Research 26 (1990) 253–258.

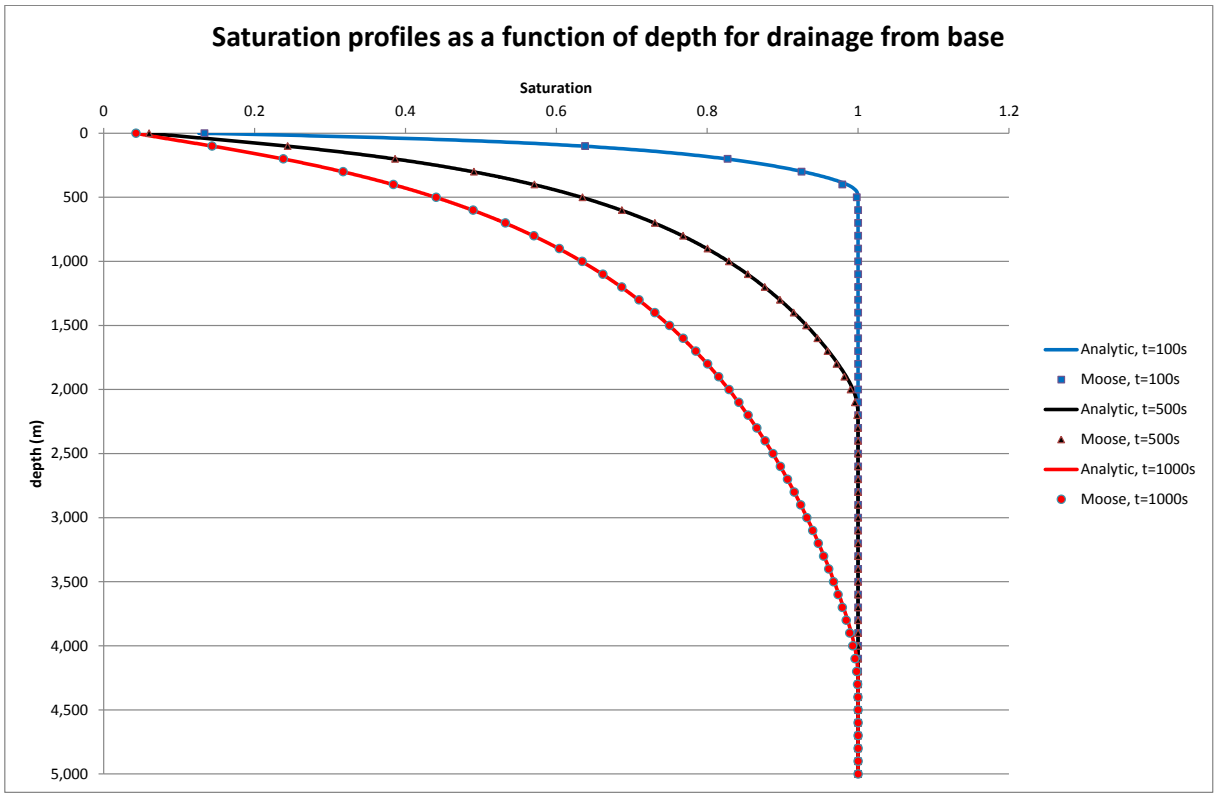

Figure 8.1: Comparison of the Warrick, Lomen and Islas analytical solution with the MOOSE solution for 3 times. This figure is shown in the standard format used in the literature: the top of the model is depth = 0 surface, and gravity acts downwards in this figure, with fluid draining from depth = ∞.

9 Infiltration and drainage

Forsyth, Wu and Pruess[1] describe a HYDRUS simulation of an experiment involving infiltration (experiment 1) and subsequent drainage (experiment 2) in a large caisson. The simulation is effectively one dimensional, and is shown in Figure 9.1.

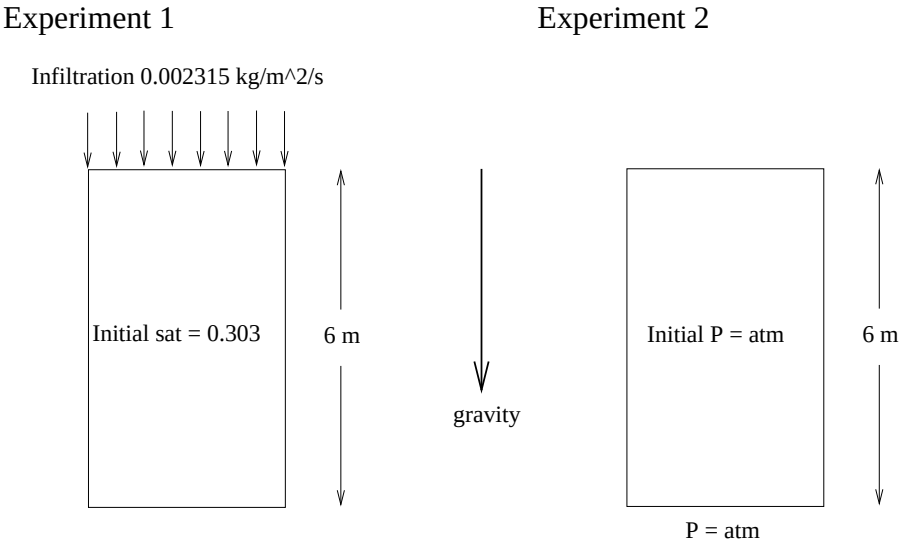

Figure 9.1: Two experimental setups from Forsyth, Wu and Pruess. Experiment 1 involves infiltration of water into an initially unsaturated caisson. Experiment 2 involves drainage of water from an initially saturated caisson.

The properties common to each experiment are:

[1] PA Forsyth, YS Wu and K Pruess, "Robust numerical methods for saturated-unsaturated flow with dry initial conditions in heterogeneous media", Advances in Water Resources 18 (1995) 25–38

Caisson	0.33
Caisson permeability	$2.95 \times 10^{-13}\,\mathrm{m}^2$
Gravity	$10\,\mathrm{m.s}^{-2}$
Water density	$1000\,\mathrm{kg.m}^{-3}$
Water viscosity	0.00101 Pa.s
Water bulk modulus	20 MPa
Water immobile saturation	0.0
Water residual saturation	0.0
Air residual saturation	0.0
Air pressure	0.0
van Genuchten α	$1.43 \times 10^{-4}\,\mathrm{Pa}^{-1}$
van Genuchten a	0.336
van Genuchten_1 cutoff	0.99

In each experiment 120 finite elements were used along the length of the Caisson. The modified van-Genuchten relative permeability curve was employed in order to improve convergence significantly. Hydrus also uses a modified van-Genuchten curve, although I couldn't find any details on the modification.

In experiment 1, the caisson is initially at saturation 0.303 ($P = -72620.4\,\mathrm{Pa}$), and water is pumped into the top with a rate $0.002315\,\mathrm{kg.m}^{-2}.\mathrm{s}^{-1}$. This causes a front of water to advance down the caisson. Figure 9.2 shows the agreement between MOOSE and the published result (this result was obtained by extracting data by hand from online graphics).

In experiment 2, the caisson is initially fully saturated at $P = 0$, and the bottom is held at $P = 0$ to cause water to drain via the action of gravity. Figure 9.2 shows the agreement between MOOSE and the published result.

Experiment 1 and the first 4 simulation days of experiment 2 are marked as "heavy" in the Richards' test suite since the simulations take around 3 seconds to complete. This means they are not run by default every time the code is updated, and must be run manually. However, the final 96 days of experiment 2 run quickly and are part of the automatic test suite.

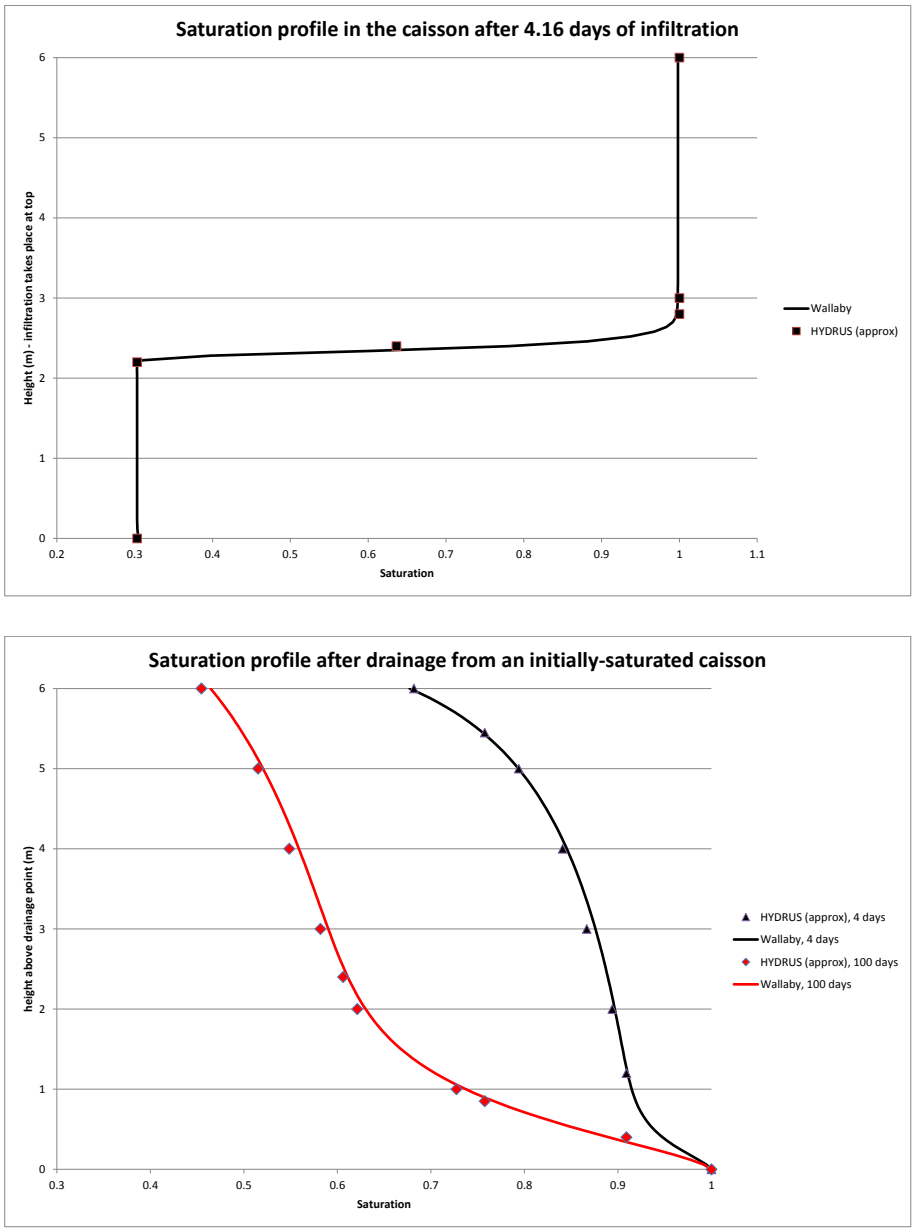

Figure 9.2: Saturation profiles in the caisson. Top: After 4.16 days of infiltration. Bottom: After drainage from an initially-saturated simulation (4 days and 100 days profiles). Note that the HYDRUS results are only approximate as I extrated the data by hand from online graphics.

10 Buckley-Leverett

MOOSE compared with a simple one dimensional Buckley-Leverett problem[1]. The single-phase fluid moves in a region $0 \leq x \leq 15\,\mathrm{m}$. A fully-saturated front initially sits at position $x = 5$, while the region $x > 5$ is initially unsaturated. With zero suction function $P_c = 0$, there is no diffusion of the sharp front, and it progresses towards the right. This is a difficult problem to simulate numerically as maintaining the sharp front is hard. The front's speed is independent of the relative permeability, since the fluid is flowing from a fully-saturated region (where $\kappa_{\mathrm{rel}} = 1$). This problem is therefore a good test of the upwinding.

In the simulation below, the pressure at the left boundary is kept fixed at $P_0 = 0.98\,\mathrm{MPa}$, while the right boundary is kept fixed at $P_{15} = -20000\,\mathrm{Pa}$, so the difference is 1 MPa. The medium's permeability is set to $\kappa = 10^{-10}\,\mathrm{m}^2$ and its porosity is $\phi = 0.15$. It is not possible to use a zero suction function in the MOOSE implementation, but using the van Genuchten parameters $\alpha = 10^{-4}\,\mathrm{Pa}^{-1}$ and $m = 0.8$ approximates it. The fluid viscosity is $\mu = 10^{-3}\,\mathrm{Pa.s}$.

The initial condition is

$$P(t=0) = \begin{cases} P_0 - (P_0 - P_{15})x/5 & \text{for } x < 5 \\ P_{15} & \text{for } x \geq 5 \end{cases} , \tag{10.1}$$

which is shown in Figure 10.1. With the suction function defined above this gives

$$S(t=0) = \begin{cases} 1 & \text{for } x \leq 4.9 \\ 0.061 & \text{for } x \geq 5 \end{cases} \tag{10.2}$$

Good approximations for the pressure $P(x,t)$ and the front position $f(t)$ may be determined from

$$\begin{aligned} \frac{\mathrm{d}f}{\mathrm{d}t} &= -\frac{\kappa}{\phi\mu}\left.\frac{\partial P}{\partial x}\right|_{x=f} , \\ P(x,t) &= \begin{cases} P_0 - (P_0 - P_{15})x/f & \text{for } x \leq f \\ P_{15} & \text{for } x > f \end{cases} , \end{aligned} \tag{10.3}$$

which has solution

$$f(t) = \sqrt{f(0)^2 + \frac{2\kappa}{\phi\mu}(P_0 - P_{15})t} . \tag{10.4}$$

For the parameters listed above, the front will be at position $f = 9.6\,\mathrm{m}$ at $t = 50\,\mathrm{s}$. This solution is only valid for zero capillary suction. A nonzero suction function will tend to diffuse the sharp front.

[1] SE Buckley and MC Leverett (1942) "Mechanism of fluid displacements in sands". Transactions of the AIME **146** 107–116

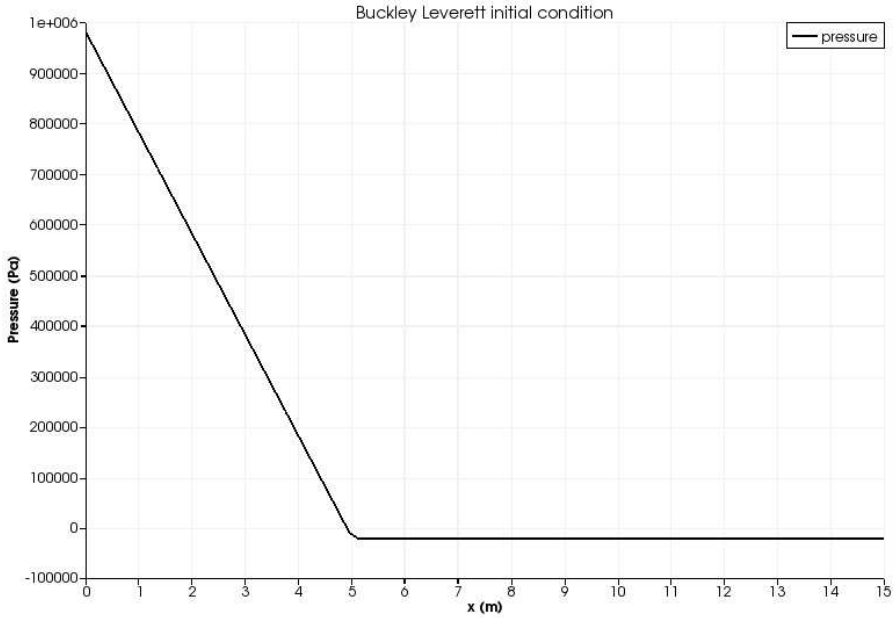

Figure 10.1: Initial setup of the Buckley-Leverett problem where porepressure is a piecewise linear function. The region $x \leq 4.9$ is fully saturated, while the region $x > 5$ has saturation 0.061. During simulation the value $P(x = 0) = 0.98 \times 10^6$ MPa is held fixed.

With coarse meshes it is impossible to simulate a sharp front, of course, since the front is spread over at least one element. It is therefore quite advantageous to use mesh adaptivity in this test, since the mesh can be fine around the front where all the interesting dynamics occurs, and coarse elsewhere.

Figure 10.2 shows the results from a MOOSE simulation with an initial mesh of element size 1 m, and a minimum size of 0.125 m, with a maximum timestep of 0.3 s. (Reducing the minimum element size or the maximum timestep size keeps the front sharper.) The front in this simulation is between $x = 9.9$ m and $x = 10.35$ m, in fair agreement with the predicted value of 9.6 m.

The automatic test suite contains a simulation with elements of size 0.1 m using a timestep of 2 s, which gives results very similar to those shown in Figure 10.2.

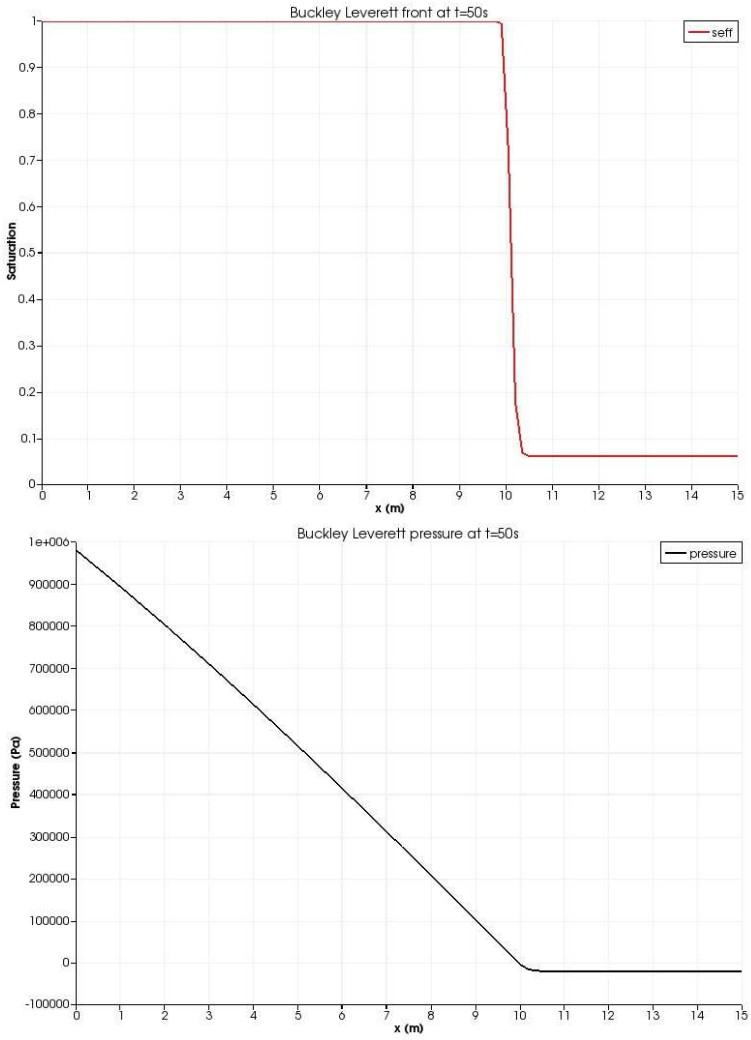

Figure 10.2: The Wallaby solution of the Buckley-Leverett problem at $t = 50\,\mathrm{s}$. Top: saturation. Bottom: porepressure. The front sits between $x = 9.9\,\mathrm{m}$ and $x = 10.35\,\mathrm{m}$.

11 Unsaturated flow in a bar - NEEDS UPDATE

This problem is one of cosflow's benchmark problems. Water inside a porous "bar" of material length 10m, and width and depth 1m is initialised to porepressure $P_0 < 0$, corresponding to water saturation $S_0 < 1$. The porepressure left-hand end (at $x = 0$) is raised and fixed at $P_1 < 0$, corresonding to water saturation S_1 with $S_0 < S_1 < 1$, and the evolution of porepressure at the right-hand end ($x = 10\,\mathrm{m}$) is recorded. Apart from the left-hand end, the other boundaries of the bar are impermeable. The setup is shown in Figure 11.1.

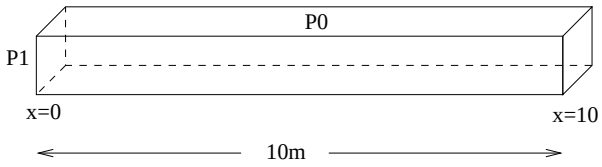

Figure 11.1: The unsaturated problem involves a porous "bar" of material of length 10m with initial porepressure P_0. The left-hand end is raised to porepressure P_1 and held fixed. The other parts of the bar's exterior surface are impermeable.

This problem exhibits quite severe mesh dependency, and since the upwinding in cosflow and Wallaby are different, the results are not expected to be the same, except in the limit of zero element size.
The following parameters are used

Bar porosity	0.1
Bar permeability	$10^{-12}\,\mathrm{m}^2$
Gravity	0
Water density	$1000\,\mathrm{kg.m}^{-3}$
Water viscosity	0.001 Pa.s
Water bulk modulus	2 GPa
Water immobile saturation	0.0
Water residual saturation	0.0
Air residual saturation	0.0
van Genuchten α	$10^{-4}\,\mathrm{Pa}^{-1}$
van Genuchten a	0.35
Initial porepressure P_0	-197347.0503 Pa
Initial saturation S_0	0.2
Applied pressure P_1	-9283.000501 Pa
Applied saturation S_1	0.8

Figure 11.2 shows agreement between Wallaby and cosflow for a variety of different mesh densities, including an adaptive mesh example. The Wallaby results appear to be closer to the zero-element-size result than cosflow, but for low mesh density exhibit spurious oscillations as the high saturation region moves into the low saturation region. (This oscillation is almost definitely due to my current inability to lump the mass term.)

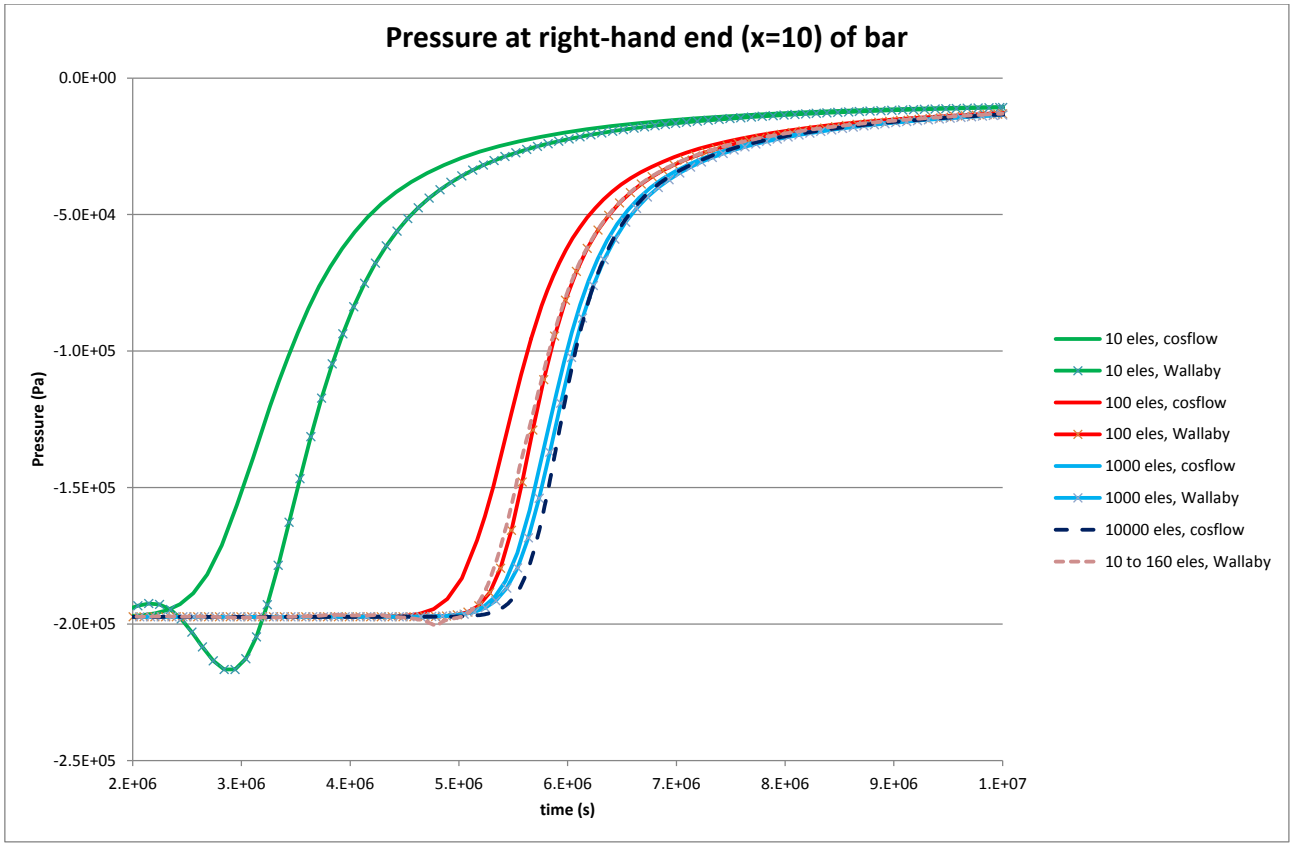

Figure 11.2: The porepressure at the right-hand end ($x = 10$) of the bar as a function of time for various different meshes.

12 Future tests

See ”Benchmarking of Richards Model” Yanlian Du, Wenqing Wang and Olaf Kolditz for a summary of the usual suspects.

See Forsyth, Wu and Pruess for more tests.